Quantification of the atomic hydrogen flux as a function of filament temperature and H_2 flow rate

D. Ugur,[a] A. J. Storm, and R. Verberk
TNO, Stieltjesweg 1, 2628 CK, Delft, The Netherlands

J. C. Brouwer and W. G. Sloof
Delft University of Technology, Department of Materials Science and Engineering, Mekelweg 2, 2628 CD Delft, The Netherlands

(Received 29 December 2011; accepted 17 March 2012; published 5 April 2012)

An isothermal sensor is developed to quantify the atomic hydrogen flux on a surface, which can be located at any distance from the molecular hydrogen cracking unit. This flux is determined from the measured heat effect due to recombination of atomic hydrogen at the sensor surface. The temperature of the sensor was kept constant at 350 °C to keep the heat losses constant during the measurement. Other heat flows due to radiative, conductive, and convective phenomena were quantified with targeted measurements. The design of the sensor allows ample area for the atomic hydrogen recombination reaction; thus enabling the flux values to be determined with high accuracy (errors were between $\pm 8.3 \times 10^{15}$ and $\pm 3.3 \times 10^{16}$ at $cm^{-2}\,s^{-1}$). The atomic hydrogen flux, generated with a commercial atomic hydrogen source was measured as a function of the filament temperature in the range of 1400 − 1950 °C and H_2 gas flow in the range of 7.44×10^{-6} to 7.44×10^{-5} mol/s (10–100 sccm). These measurements showed that the atomic hydrogen flux increases with both filament temperature and H_2 flux. © *2012 American Vacuum Society*. [http://dx.doi.org/10.1116/1.3700231]

I. INTRODUCTION

Exposure of surfaces to atomic hydrogen is a well established surface cleaning technique that can efficiently remove carbon deposits and surface oxides from metals[1,2] and semiconductors.[3–5] Recently this technique is also being considered for Si etching in nanopatterning studies[6] and for extreme ultraviolet lithography (EUVL) systems to sustain the cleanliness of the reflective optics. Removal of photon-induced carbon contamination and surface oxidation through exposure to atomic hydrogen has been demonstrated experimentally.[7–12] A number of methods are available in the literature to generate atomic hydrogen radicals: RF discharge plasma,[13,14] microwave discharge decomposition,[15,16] and thermal cracking using either a hot capillary[17,18] or a hot wire.[7,19,20] Thermal cracking appears to be the most promising method for EUVL applications, because it causes less damage in the case of overcleaning.[11,12,14]

A high flux of atomic hydrogen is required to obtain a sufficient cleaning rate on the contaminated surfaces. To determine the kinetics and efficiency of the process, it is imperative to quantify the number of atomic hydrogen species incident on the surface; however, this is not a straightforward task. To this end, multiple techniques are available: laser-induced fluorescence,[20,21] resonance enhanced multiphoton ionization,[22] molecular beam mass spectrometry,[23,24] detection of the current generated due to electron/hole pair creations in a material,[25] and the detection of the recombinative heating of H radicals on a catalytic probe.[26–31] Of these techniques, the catalytic probe method was employed in our research, since it quantifies the atomic hydrogen flux on a surface rather than its concentration. Moreover, utilizing the catalytic probe method does not require significant investments.

The catalytic probe approach is also used in microcalorimetry studies, where atoms and molecules effuse through an orifice and recombine on the walls of a calorimeter box.[26] Instead of these boxes, UHV compatible thermocouple junctions[27–30] are also employed, allowing positioning flexibility in the measurements. The recombinative heating effect on a catalytically active surface is determined from a heat balance by precisely measuring the incident cooling and heating effects at steady state. From this value, the amount of recombining atomic hydrogen species is determined, which is proportional to the incoming flux. Active stabilization of the sensor temperature ensures that the material properties and reaction kinetics do not vary during measurements.[31] A heat balance on the sensor surface is adopted, which is commonly employed in hydrogen dissociation studies.[31–35]

The atomic hydrogen sensors mentioned previously exhibit high uncertainty levels in the measurements[30] and mostly require thermal shielding to block the radiative heating from the hydrogen gun.[12,31,36] In the present study, it will be shown that an isothermal atomic hydrogen sensor provides sufficient precision in determining the atomic hydrogen flux values and the device operates without the necessity of a radiation shielding in the chamber. This precision is reached by careful quantification of all relevant heat fluxes into and out of the sensor.

The sensor was used to determine the effects of filament temperature and H_2 flow on the atomic hydrogen flux. First, the theoretical background of the determination of the atomic hydrogen flux with an isothermal catalytic sensor will be discussed briefly. Next, the atomic hydrogen flux measured as a function of pressure and flow will be reported.

[a]Electronic mail: d.ugur@tudelft.nl

Finally, the accuracy of the atomic hydrogen flux measurements and the main findings of this study will be discussed.

II. THEORY

The determination of the flux of atomic hydrogen using a catalytic probe relies on the exothermic recombination reaction that proceeds at a platinum surface:

$$H + H \rightarrow H_2. \quad (1)$$

The flux of atomic hydrogen particles (ϕ_H) on the sensor surface can be calculated by measuring the heat load on the sensor due to the recombination reaction ($\dot{Q}_{\text{rec}}$) as

$$\phi_H = \frac{2N_A\dot{Q}_{\text{rec}}}{A_{\text{Pt}}\gamma\Delta H_H}. \quad (2)$$

Here N_A is the Avogadro number (6.02×10^{23} mol^{-1}), A_{Pt} is the area of the sensor surface, ΔH_H is the heat of recombination [cf. Eq. (1)] and equals -435.94 kJ/mol H_2 (see Ref. 37), and γ is the recombination coefficient.

The sensor temperature is kept constant during all measurements and the power required to keep it at that temperature is recorded continuously. The heat load on the sensor due to recombination of atomic hydrogen species is calculated from the power input to the sensor surface ($\dot{Q}_{\text{in}}$), using the steady-state heat balance as depicted in Fig. 1. Hence:

$$\dot{Q}_{\text{rec}} = \dot{Q}_{\text{cond}} + \dot{Q}^{\text{out}}_{\text{rad}} + \dot{Q}^{\text{H}_2}_{\text{gas}} - \dot{Q}^{\text{in}}_{\text{rad}} - \dot{Q}_{\text{in}}. \quad (3)$$

Conductive heat loss through the leads ($\dot{Q}_{\text{cond}}$) and the radiative heat loss from the sensor to the ambient ($\dot{Q}^{\text{out}}_{\text{rad}}$) are measured cumulatively and this value is constant throughout the experiments. The term $\dot{Q}^{\text{H}_2}_{\text{gas}}$ denotes the convective heat transfer of the sensor with the surrounding hydrogen flow and $\dot{Q}^{\text{in}}_{\text{rad}}$ refers to the radiative heat load from the filament to the sensor surface.

In order to quantify the magnitude of each heat transfer term in Eq. (3), the following targeted measurements were performed: (i) The values for $\dot{Q}_{\text{cond}}$ and $\dot{Q}^{\text{out}}_{\text{rad}}$ are determined in the absence of a gas flow (i.e., at the base pressure) and without atomic hydrogen source operation. (ii) The value for the radiative heating $\dot{Q}^{\text{in}}_{\text{rad}}$ is determined at the base pressure, but this time with the filament turned on. This heating effect is significant since the atomic hydrogen source used in our experiments is operated with a hot tungsten filament. (iii) To determine $\dot{Q}^{\text{H}_2}_{\text{gas}}$, the ratio of the heat transfer effects between He and H_2 flows (k) is determined initially. This is done separately for each flow rate of He and H_2 without powering up the filament. Next, the measurements with He are repeated with the filament on to determine the convective cooling effects in the presence of a hot filament. The system configuration during the measurements to determine the terms in the heat balance is summarized in Table I and the quantification of the terms is provided in the results section.

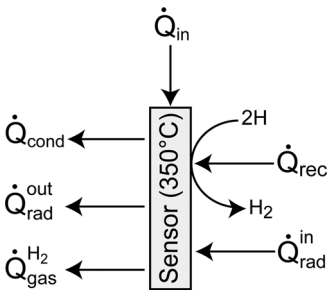

FIG. 1. Heat balance at the sensor surface to determine the recombinative heating effects ($\dot{Q}_{\text{rec}}$). Here $\dot{Q}_{\text{in}}$ is the power input and $\dot{Q}_{\text{cond}}$, $\dot{Q}^{\text{out}}_{\text{rad}}$, $\dot{Q}^{\text{H}_2}_{\text{gas}}$ terms are the conductive, radiative, and convective losses from the sensor surface to the surroundings, respectively. $\dot{Q}^{\text{in}}_{\text{rad}}$ is the radiative heat input from the cracking gun.

TABLE I. Experimental conditions to determine the heat effect due to the recombination of atomic hydrogen ($\dot{Q}_{\text{rec}}$) at the Pt sensor surface. $\dot{Q}_{\text{cond}}$, $\dot{Q}^{\text{out}}_{\text{rad}}$, and $\dot{Q}^{\text{H}_2}_{\text{gas}}$ denote the conductive, radiative, and convective losses from the sensor to the ambient, $\dot{Q}^{\text{in}}_{\text{rad}}$ is the radiative heat input from the atomic hydrogen source, and k is the ratio of the heat transfer effects between H_2 and He gases.

He flow	H_2 flow	H source	Evaluated terms
off	off	off	$\dot{Q}_{\text{cond}} + \dot{Q}^{\text{out}}_{\text{rad}}$
on	off	off	k
off	on	off	
off	off	on	$\dot{Q}^{\text{in}}_{\text{rad}}$
on	off	on	$\dot{Q}^{\text{H}_2}_{\text{gas}}/k$
off	on	on	$\dot{Q}_{\text{rec}}$

III. EXPERIMENT

A schematic representation of the experimental system is shown in Fig. 2. The sensor is located at 120 mm from the front of the atomic hydrogen source and the surface normal of the sensor is oriented towards this gun. The sensor is made of a 0.025 mm thick rectangular Pt foil (99.95% pure, Goodfellow) of 30×5 mm^2 size. The Pt leads (99.99% pure, Goodfellow) with a diameter of 0.5 mm are spot welded to the sensor. These wires deliver the power for resistive heating and support the foil. The surface area of the Pt sensor was chosen such that it is sufficiently large to realize a high number of atomic hydrogen recombinations, resulting in a high signal to noise ratio. A much larger sensor area is not recommended though, because temperature gradients in the sensor surface will complicate the analysis.

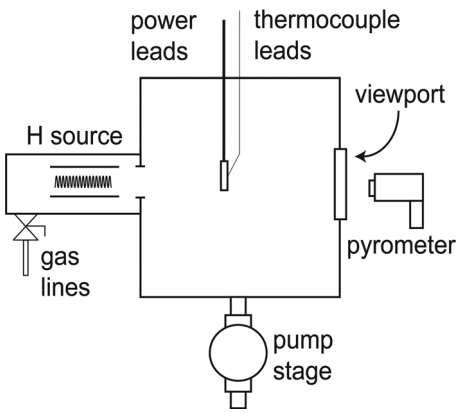

FIG. 2. Illustration of the experimental setup.

The sensor temperature is kept constant at 350 °C by a PID regulated power supply (Delta, ES030-10), which provides the resistive heating of the foil. The temperature of the sensor is measured with a K type thermocouple (made of 0.2 mm diameter wires) spot welded to the backside of the Pt foil (i.e., the side facing away from the atomic hydrogen source). To prevent stray recombinative heating, the Pt power leads and the thermocouple wires are shielded with Teflon and fused silica tubing, respectively. Prior to each set of experiment, the foil was degassed thoroughly at 400 °C to provide a clean metal surface.

A commercial H_2 cracker (Veeco Atomic Hydrogen Source) was used to generate the atomic hydrogen. The gun is equipped with a tungsten filament inside a tube and the H_2 molecules are dissociated thermally as they are purged over this filament. The filament of the gun was degassed and stabilized at the operation temperature prior to operation.

The temperature of the filament was measured with a two-color pyrometer (Raytek Marathon series MR1SC) through a glass viewport. The pyrometer was calibrated by the Dutch Metrology Institute (VSL) against a blackbody reference according to ITS-90.[38] The two-color mode was employed during the measurements to determine the temperature of the filament from the ratio of two separate and overlapping infrared bands (i.e., 0.75–1.1 μm and 0.95–1.1 μm). To correct for the wavelength dependence of emissivity, the emissivity-slope parameter was set to 1.06, which is the recommended value for tungsten by the manufacturer. The filament temperature was repeatable to ±6 °C (within 95% confidence) during the span of measurements. The main purpose of the pyrometer usage was to ensure that the filament is maintained at the same temperature during the atomic hydrogen recombination experiment and the prior targeted measurements (to determine the radiative and convective heat effects). Hence a small systematic error in the temperature measurements, which cannot be ruled out, has no direct impact on the accuracy of the atomic hydrogen flux quantification.

Hydrogen or helium gas (both 99.999% pure) was fed to the chamber through the gun and the gas flows were controlled by calibrated mass-flow controllers (Bronkhorst EL Flow type). The power supply of the gun was adjusted for each experiment because filament temperature depends both on the drive current and the vacuum conditions. The measurements were carried out with various filament temperatures in the range of 1400 – 1950 °C and constant gas flows in the range of 7.44×10^{-6} to 7.44×10^{-5} mol/s (10–100 sccm).

The base pressure (below 1×10^{-8} mbar) of the vacuum chamber was measured with a compact full range pressure gauge (Pfeiffer PKR251), whereas for the measurements with the gas, an active capacitive transmitter (Pfeiffer CMR365) was used. The latter gauge allows high accuracy measurements (0.5% of the readings) independent of the nature of the gas.

The pumping circuit employed in the system consists of a turbomolecular pump (Pfeiffer HiPace 700), backed with an oil free piston vacuum pump (Pfeiffer, XtraDry 150-2). Effective pump speed is 550 and 650 l/s for H_2 and He, respectively. In order to attain the same chamber pressure with He compared to the measurements with H_2 at a given flow rate, the rotation frequency of the turbomolecular pump was lowered during the He experiments. Table II lists the pressures, pump frequencies and gas flows applied in the experiments.

TABLE II. Overview of the pressure, pump rotation frequency, and gas flow rates used in the experiments.

Pressure	Pump frequency (Hz)		Gas flow	
(mbar)	H_2	He	(sccm)	(mol/s)
1×10^{-1}	410	287	100	7.44×10^{-5}
1×10^{-2}	533	410	65	4.84×10^{-5}
1×10^{-3}	820	820	20	1.49×10^{-5}
5×10^{-4}	820	820	10	7.44×10^{-6}

IV. RESULTS AND DISCUSSION

A. Elements of the heat balance

1. Radiative and conductive heat losses

The measurement with the isothermal sensor at the base pressure shows that 0.420 ± 0.002 W is lost to the cumulative effect of radiative and conductive cooling (i.e., $\dot{Q}_{\mathrm{rad}}^{\mathrm{out}}$ and $\dot{Q}_{\mathrm{cond}}$) without the atomic hydrogen gun in operation. The magnitude of this loss is constant throughout the experiments, since the sensor temperature is fixed, the leads are shielded against stray heating and the measurements were executed at steady state. The chamber wall temperatures at different locations were also measured during the experiments; the change in the radiative cooling rate of the sensor due to wall temperature fluctuation appeared to be negligible during the measurements.

2. Heat losses by convection in the gas

The convective heat transport from the sensor to the surrounding gas has a significant effect on the heat balance, especially at higher pressures. To quantify this loss, He was used instead of H_2, because with the latter the heat transport effects due to the gas flow and atomic hydrogen recombination cannot be separated. This procedure is similar to that reported earlier[32–35,39] where the H_2 cracking experiments were conducted first with He to measure the convective cooling of the filament due to the flowing gas. Next, the measured effect was adapted to H_2 to account for the differences between the two gases.[32]

In this study, that approach was improved further by initially determining the convective cooling of the sensor in H_2 and He flows, respectively. The exact ratio (k) between those cooling rates (i.e., H_2 to He) was determined for each flow (and thus pressure) applied, since this ratio appears to depend on pressure. Targeted measurements were carried out by flowing H_2 and He separately at the corresponding flow rates (cf. Table II) and observing the convective cooling effect due to the heat transfer from the sensor to the surrounding gas. During these measurements, the filament of the H_2 cracker was not powered. From these measurements it followed that the

convective cooling of the sensor due to the H_2 flow, was about twice the magnitude of the cooling effect observed due to the He flow. Thus the ratio k is about 2.

By repeating the measurements with He, but now with the filament on, the convective cooling effect due to He flow in the presence of a hot filament ($\dot{Q}_{\text{gas}}^{\text{He}}$) was measured. From this value, the convective cooling effect due to H_2 flow during the recombination experiments were calculated using the previously determined k ratio according to

$$\dot{Q}_{\text{gas}}^{\text{H}_2} = k \cdot \dot{Q}_{\text{gas}}^{\text{He}}. \tag{4}$$

This method is valid, provided that the gas composition at the vicinity of the sensor is similar for the targeted measurements and the recombination experiments with hydrogen. In the recombination experiments, the gas is mainly composed of H_2 near the sensor. For example, in the experiment with the highest atomic hydrogen flux (i.e., with 1950 °C filament temperature and 7.44×10^{-5} mol/s (100 sccm) H_2 flow rate), it is estimated that the gas contained less than 1% atomic hydrogen near the sensor.

The cooling effect as a function of the H_2 flow rate is depicted in Fig. 3. This effect depends on the flow rate, but is not affected by the filament temperature of the H_2 cracker. The results pertaining to the measurements with He showed that no heat was carried from the filament to the sensor by the flowing gas, since the magnitude of the cooling effect remained unchanged when the filament was turned on or off. Thus an increased flow of H_2 may be beneficial to minimize the heat load to the optics when cleaning with atomic hydrogen.

3. Radiative heat input

Atomic hydrogen species are generated by purging H_2 gas over a hot tungsten filament, where the molecules are dissociated thermally.[19] This requires filament temperatures in excess of 1800 °C.[34] When the filament is heated to such high temperatures, there is an additional heat load imposed on the sensor surface ($\dot{Q}_{\text{rad}}^{\text{in}}$) due to the thermal radiation. Assuming that the filament and the sensor are gray bodies and the filament radiates diffusely, this radiative heat load can be written as

$$\dot{Q}_{\text{rad}}^{\text{source}} = A_{\text{Pt}} \varepsilon_{\text{Pt}}(T_{\text{Pt}}) \varepsilon_{\text{W}}(T_{\text{W}}) F \sigma T_{\text{W}}^4. \tag{5}$$

Here $\varepsilon_{\text{Pt}}(T_{\text{Pt}})$ is the emissivity of the Pt surface at the sensor temperature (T_{Pt}= 350 °C), $\varepsilon_{\text{W}}(T_{\text{W}})$ is the emissivity of tungsten at the corresponding hot wire filament temperature (T_{W}), F is the radiative viewing factor between the two surfaces, and σ is the Stefan–Boltzmann constant (5.670373×10^{-8} W m^{-2} K^{-4}). The sensor is held at a constant temperature; thus $\varepsilon_{\text{Pt}}(T_{\text{Pt}})$ stays constant throughout the measurements. However, a range of hot wire filament temperatures (T_{W}) was applied when determining the atomic hydrogen flux. Then, a corresponding value for the emissivity of tungsten $\varepsilon_{\text{W}}(T_{\text{W}})$ must be taken.[40]

The emissivity of the tungsten depends on the wavelength as well as temperature; thus the gray body assumption in Eq. (5) is not applicable. Moreover the calculation of the viewing factors is rather cumbersome. Therefore the magnitude of the total radiative heat load is determined experimentally at the base pressure as a function of the hot wire filament temperature (Fig. 4). This heat effect is a combination of the contributions from the two hot components of the gun, viz. the filament and the indirectly heated gas conductance tube; see Fig. 2.

4. Recombinative heat input

The magnitude of the recombinative heating was determined by inserting the aforementioned heat loads (i.e., $\dot{Q}_{\text{rad}}^{\text{out}}$, $\dot{Q}_{\text{cond}}$, $\dot{Q}_{\text{gas}}^{\text{H}_2}$, and $\dot{Q}_{\text{rad}}^{\text{in}}$) into the heat balance according to Eq. (3). The recombinative heat load as a function of hot wire filament temperature for different H_2 gas flows is presented in Fig. 5.

The recombinative heat load depends exponentially on the filament temperature and is proportional to the H_2 flow. The maximum recombinative heating effect was measured at 1950 °C filament temperature with a H_2 flow rate of 7.44×10^{-5} mol/s (100 sccm). Then the magnitude of the recombinative heating is roughly 45% of the radiative load

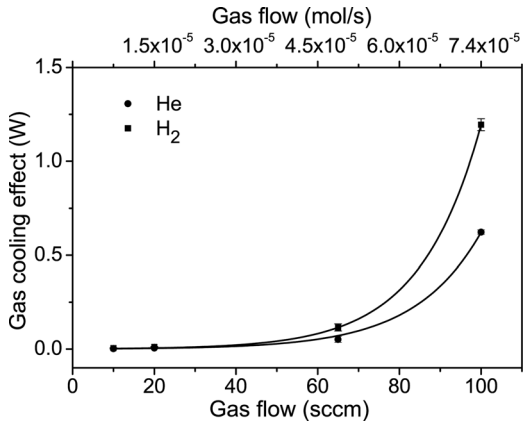

FIG. 3. Convective cooling of the Pt isothermal sensor operating at 350 °C as a function of the H_2 and He gas flow rate. Solid lines represent a nonlinear fit to the data.

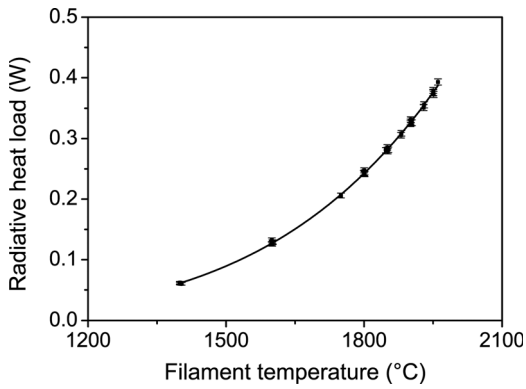

FIG. 4. Total radiative heating effect incident on the Pt sensor surface as a function of the hot wire filament temperature of the H_2 cracker. Sensor is operated at 350 °C and the measurements were performed at the base pressure ($< 1 \times 10^{-8}$ mbar). Solid line represents a nonlinear fit to the data.

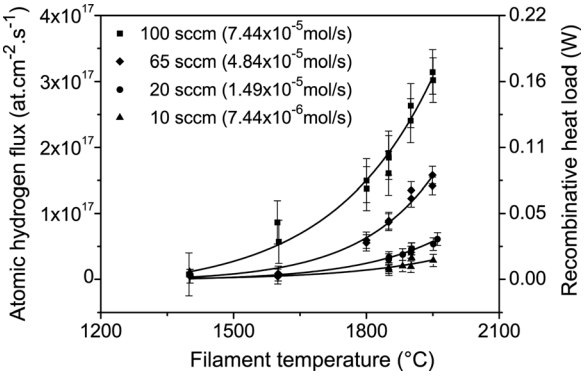

FIG. 5. Atomic hydrogen flux at the sensor surface as a function of the hot-wire filament temperature, for different H_2 flow rates. The atomic hydrogen flux is determined from the recombinative heat load (indicated with the right-hand vertical axis). Solid lines represent a nonlinear fit to the data.

and is about 22% of the convective load due to the H_2 flow. Table III lists the typical magnitudes of the heat balance terms, specific to this operation condition (1950 °C filament temperature and 7.44×10^{-5} mol/s (100 sccm) H_2 flow).

B. Quantification of the atomic hydrogen flux

The number of atomic hydrogen particles incident per unit of sensor area and per unit of time (atomic hydrogen flux) was calculated with Eq. (2). It is assumed that all the energy generated due to the recombination reaction is fully transmitted to the sensor surface. Moreover, the recombination probability of atomic hydrogen on Pt (γ_{Pt}) is taken equal to unity, i.e., all of the atomic hydrogen species that reach the sensor surface will recombine directly.

The literature regarding the atomic hydrogen recombination probability (γ_{Pt}), however, gives contradicting values.[27,32,41–43] The reported values vary from 0.03 to 1. A study by Livshits *et al.*[43] indicates that these inconsistencies are caused by different cleanliness of the metal surfaces, but for a clean metal surface the recombination coefficient equals 1. As the Pt sensor in our research was always degassed prior to each measurement, the value taken for γ_{Pt} as 1 is well justified. It is noted that a lower recombination probability leads to higher value for the atomic hydrogen flux.

The atomic hydrogen flux as a function of the filament temperature for different H_2 flow rates are depicted in Fig. 5. The flux increases exponentially with the filament temperature, which is in agreement with the previous findings regarding H_2 cracking and recombination studies.[31,39,44] Such exponential dependence on filament temperature can be explained by the H_2 dissociation at the hot filament surface being a thermally activated process.[34,35,44,45]

A promising result in view of application of atomic hydrogen for cleaning surfaces (e.g., optics) is that the radical flux increases proportionally with the H_2 flow rate through the gun. The relationship between the H_2 flow rate and the atomic hydrogen flux detected at the sensor surface is shown in Fig. 6(a). It can be seen that the radical flux increases linearly with the H_2 flow up to 4.84×10^{-5} mol/s (65 sccm). However when the H_2 flow rate is further increased to 7.44×10^{-5} mol/s (100 sccm), an additional flux of atomic hydrogen is observed with respect to a proportional increase of the flux with the H_2 flow rate. An increasing H_2 flow rate is accompanied with a significant rise in the chamber pressure [see Fig. 6(b)], which leads to even higher pressures at the vicinity of the hot filament. Thus, the number of collisions with the filament surface increases accordingly and the generation of atomic hydrogen is promoted. It is noted that in this study, the pressure is still low enough to neglect the gas phase three-body recombination of H radicals.[46] At the highest pressure (0.1 mbar), the number of radicals lost due to three-body recombination during their travel from the gun to the sensor is two orders of magnitude smaller than the number of radicals detected at the sensor, per second.

TABLE III. Typical heat loads observed during sensor operation in 7.44×10^{-5} mol/s (100 sccm) H_2 flow and 0.1 mbar pressure. The sensor and the cracking filament are maintained at 350 and 1950 °C, respectively. $\dot{Q}_{cond}$, $\dot{Q}_{rad}^{out}$, and $\dot{Q}_{gas}^{H_2}$ denote the conductive, radiative, and convective losses from the sensor to the ambient. $\dot{Q}_{rad}^{in}$ and $\dot{Q}_{rec}$ denote the radiative and recombinative heat inputs to the sensor.

Heat transfer terms	Magnitude (W)
$\dot{Q}_{cond} + \dot{Q}_{rad}^{out}$	0.578
$\dot{Q}_{rad}^{in}$	0.384
$\dot{Q}_{gas}^{H_2}$	0.785
$\dot{Q}_{rec}$	0.171

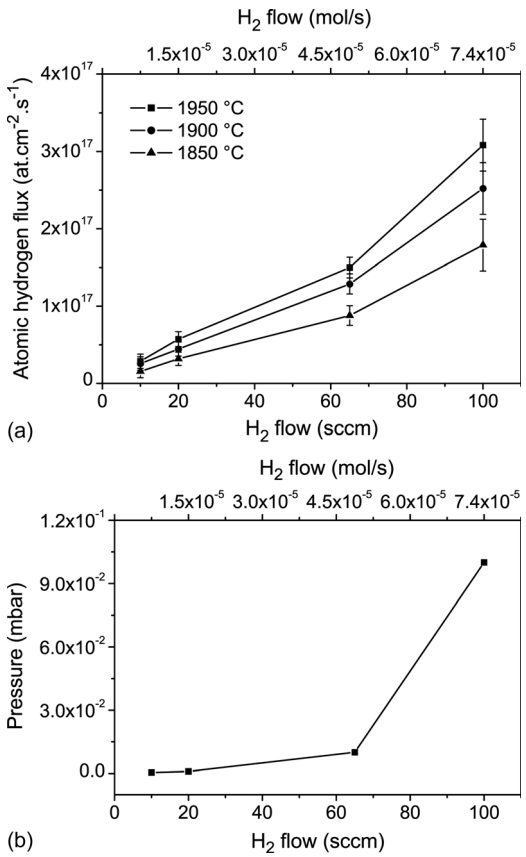

FIG. 6. (a) Atomic hydrogen flux at the sensor surface as a function of the H_2 flow rate through the gun, (b) chamber pressure as a function of the H_2 flow rate.

For cleaning applications, the number of hydrogen radicals in the incoming beam is of concern rather than the atomic to molecular hydrogen ratio. Our study shows that even though the cracking efficiency decreases with increasing flow rate and pressure; still the number of atomic hydrogen species arriving at the object surface rises.

The sensor developed in this study delivers highly reproducible and accurate flux measurements, as indicated in Fig. 5. In previous studies, the radical flux was either accompanied with a high uncertainty margin[30] or no accuracy was reported at all.[25,28] Moreover, the sensor developed in this study is versatile. Its configuration and positioning can be changed easily without any restrictions, because no intricate electrical contacts or delicate cooling systems[25,47] are required. Also the sensor can operate without a radiation shield and it is not required to stabilize or saturate the sensor before use.[25,47] Thus the sensor can be used to measure the H radical flux continuously or to track instantaneous changes within the flow.

V. CONCLUSIONS

An isothermal atomic hydrogen sensor was designed without a radiation shield to determine accurately an atomic hydrogen flux at a surface. This atomic hydrogen flux was determined from the observed heat of recombination while taking into account the radiative heating effect from the atomic hydrogen source, conduction through the power leads and convection by the surrounding gas. The flux was determined as a function of hot wire filament temperature of the atomic hydrogen source and molecular hydrogen flow rate.

The atomic hydrogen flux increases exponentially with the filament temperature of the source. An increase of about two orders of magnitude was observed when the filament temperature is raised from 1400 to 1950 °C.

The atomic hydrogen flux increases linearly with the hydrogen flow up to 4.84×10^{-5} mol/s (65 sccm), but at higher hydrogen flows an additional flux of radicals was observed at the sensor surface. This was attributed to the increase in the chamber pressure. With the filament at 1950 °C, an increase of the flow from 7.44×10^{-6} to 7.44×10^{-5} mol/s (10 to 100 sccm), accompanied by a pressure rise from 5×10^{-4} to 1×10^{-1} mbar, yielded one order of magnitude higher atomic hydrogen flux.

A high hydrogen flow through the gun, thus a higher pressure, creates a sufficiently high atomic hydrogen flux at the sensor surface. This provides short cycle times during atomic hydrogen cleaning of surfaces (e.g., optics). In addition, a high H_2 flow rate results in a favorable convective cooling effect leading to low thermal loads during cleaning cycles.

ACKNOWLEDGMENT

This work was supported by FP7-PEOPLE program of Marie Curie ITN, under the project name "Surface Physics for Advanced Manufacturing" (SPAM), Grant No. 215723.

[1]K. Uchida, A. Izumi, and H. Matsumura, Thin Solid Films **395**, 75 (2001).
[2]M. R. Baklanov, D. G. Shamiryan, Zs. Tokei, G. P. Beyer, T. Connard, S. Vanhaelemeersch, and K. Maex, J. Vac. Sci. Technol. B **19**, 1201 (2001).
[3]E. Schubert, N. Razek, F. Frost, A. Schindler, and B. Rauschenbach, J. Appl. Phys. **97**, 023511 (2005).
[4]G. R. Bell, N. S. Kaijaks, R. J. Dixon, and C. F. McConville, Surf. Sci. **401**, 125 (1998).
[5]A. Khatiri, T. J. Krzyzewski, C. F. McConville, and T. S. Jones, J. Cryst. Growth **282**, 1 (2005).
[6]E. Salomon, T. Angot, C. Thomas, J.-M. Layet, P. Palmgren, C. I. Nlebedim, and M. Göthelid, Surf. Sci. **603**, 3350 (2009).
[7]I. Nishiyama, H. Oizumi, K. Motai, A. Izumi, T. Ueno, H. Akiyama, and A. Namiki, J. Vac. Sci. Technol. B **23**, 3129 (2005).
[8]K. Motai, H. Oizumi, S. Miyagaki, I. Nishiyama, A. Izumi, T. Ueno, and A. Namiki, Thin Solid Films **516**, 839 (2008).
[9]S. Graham, C. Steinhaus, W. M. Clift, and L. Klebanoff, Proc. SPIE **5037**, 460 (2003).
[10]H. Oizumi, A. Izumi, K. Motai, I. Nishiyama, and A. Namiki, Jpn. J. Appl. Phys. **46**, L633 (2007).
[11]S. Graham, M. Malinowski, C. Steinhaus, P. Grunow, and L. Klebanoff, Proc. SPIE **4688**, 431 (2002).
[12]H. Oizumi, H. Yamanashi, I. Nishiyama, K. Hashimoto, S. Ohsono, A. Masuda, A. Izumi, and H. Matsumura, Proc. SPIE **5751**, 1147 (2005).
[13]C. K. Sinclair, B. M. Poelker, and J. S. Price, in Proceedings of the 1997 Particle Accelerator Conference, Vancouver, British Columbia, 1997, p. 2864.
[14]S. Graham, C. Steinhaus, W. M. Clift, and L. Klebanoff, J. Vac. Sci. Technol. B **20**, 2393 (2002).
[15]A. Donnelly, M. P. Hughes, J. Geddes, and H. B. Gilbody, Meas. Sci. Technol. **3**, 528 (1992).
[16]R. W. McCullough, J. Geddes, A. Donnelly, M. Liehrt, M. P. Hughes, and H. B. Gilbody, Meas. Sci. Technol. **4**, 79 (1993).
[17]C. Eibl, G. Lackner, and A. Winkler, J. Vac. Sci. Technol. A **16**, 2979 (1998).
[18]K. Tschersich and V. von Bonin, J. Appl. Phys. **84**, 4065 (1998).
[19]I. Langmuir, J. Am. Chem. Soc. **38**, 1145 (1916).
[20]L. Schafer, C. P. Klages, U. Meier, and K. Kohse-Honighaus, Appl. Phys. Lett. **58**, 571 (1991).
[21]A. D. Tserepi and T. A. Miller, J. Appl. Phys. **75**, 7231 (1994).
[22]F. G. Celii and J. E. Butler, Appl. Phys. Lett. **54**, 1031 (1989).
[23]S. J. Harris, A. M. Weiner, and T. A. Perry, Appl. Phys. Lett. **53**, 1605 (1988).
[24]K. G. Tschersich, J. Appl. Phys. **87**, 2565 (2000).
[25]H. Nienhaus, H. S. Bergh, B. Gergen, A. Majumdar, W. H. Weinberg, and E. W. McFarland, Appl. Phys. Lett. **74**, 4046 (1999).
[26]J. W. Fox, A. C. H. Smith, and E. J. Smith, Proc. Phys. Soc. **73**, 533 (1959).
[27]R. K. Grubbs and S. M. George, J. Vac. Sci. Technol. A **24**, 486 (2006).
[28]W. L. Gardner, J. Vac. Sci. Technol. A **13**, 763 (1995).
[29]S. J. Harris and A. M. Weiner, J. Appl. Phys. **74**, 1022 (1993).
[30]N. Tsuji, T. Akiyama, and H. Komiyama, Rev. Sci. Instrum. **66**, 5450 (1995).
[31]A. Sutoh, S. Ohta, Y. Okada, and M. Kawabe, Jpn. J. Appl. Phys. **34**, L1379 (1995).
[32]R. Gat and J. C. Angus, J. Appl. Phys. **74**, 5981 (1993).
[33]F. Jansen, I. Chen, and M. A. Machonkin, J. Appl. Phys. **66**, 5749 (1989).
[34]T. Otsuka, M. Ihara, and H. Komiyama, J. Appl. Phys. **77**, 893 (1995).
[35]X. Qi, Z. Chen, and G. Wang, J. Mater. Sci. Technol. **19**, 235 (2003).
[36]H. Nienhaus, B. Gergen, H. S. Bergh, A. Majumdar, W. H. Weinberg, and E. W. McFarland, J. Vac. Sci. Technol. A **17**, 670 (1999).
[37]P. W. Atkins, *Physical Chemistry*, 5th ed. (Oxford University Press, Oxford, 1994).
[38]H. Preston-Thomas, Metrologia **27**, 3 (1990).
[39]D. W. Comerford, J. A. Smith, M. N. R. Ashfold, and Y. A. Mankelevich, J. Chem. Phys. **131**, 044326 (2009).
[40]I. Langmuir, Phys. Rev. **7**, 302 (1916).
[41]B. J. Wood and H. Wise, J. Phys. Chem. **65**, 1976 (1961).
[42]G. A. Melin and R. J. Madix, Trans. Faraday Soc. **67**, 2711 (1971).
[43]A. I. Livshits, F. El Balghiti, and M. Bacal, Plasma Source Sci. Technol. **3**, 465 (1994).
[44]J. R. Andersox, I. M. Ritchie, and M. W. Roberts, Nature **227**, 704 (1970).
[45]G. Bryce, Proc. Cambridge Philos. Soc. **32**, 648 (1936).
[46]J. Geddes, R. W. McCullough, A. Donnelly, and H. B. Gilbody, Plasma Sources Sci. Technol. **2**, 93 (1993).
[47]V. A. Kagadei, E. V. Nefedtsev, D. I. Proskurovskii, S. V. Romanenko, and V. V. Chupin, Instrum. Exp. Tech. **51**, 142 (2008).